

International Journal of  
**Applied  
Ceramic  
TECHNOLOGY**

Ceramic Product Development and Commercialization

## **Alumina Toughened Zirconia Nanocomposite Incorporating $\text{Al}_2\text{O}_3$ Whiskers**

**A. Aguilar-Elguézabal and M. H. Bocanegra-Bernal\***

*Centro de Investigación en Materiales Avanzados, CIMAV S.C., Laboratorio Nacional de  
Nanotecnología, Miguel de Cervantes # 120, Complejo Industrial, Chihuahua 31109, México*

We investigated the Vickers hardness and fracture toughness of an  $\text{Al}_2\text{O}_{3(n)} + 70 \text{ wt\% ZrO}_2$  (TZ-3Y)<sub>n</sub> nanocomposite with addition of 2.5 wt%  $\text{Al}_2\text{O}_3$  whiskers. Densities greater than 95% were reached after conventional sintering at 1500°C. The fracture toughness was increased 62% over pure  $\text{Al}_2\text{O}_3$ . Microcracking and crack deflection can be the mechanisms responsible to improve the fracture toughness. The use of ATZ composites with a low percent of whiskers can be a promising biomedical material for medical and dental applications given its large increase in fracture toughness over pure alumina and the observed relief from aging issues of zirconia.

### **Introduction**

Oxide ceramics are gaining wide acceptance in modern technology considering the combination of properties such as hardness, refractory characteristics, resistance to aggressive media, etc.<sup>1,2</sup> In contrast, the major disadvantage of the ceramic materials is their brittle nature, characterized by the low fracture toughness.<sup>3</sup> Research works have been done focusing on the property improvement that results when alumina ( $\text{Al}_2\text{O}_3$ ) and zirconia ( $\text{ZrO}_2$ ) ceramics are combined to form

ceramic composites. The addition of one ceramic to another often produces a composite with more desirable properties than the individual components.<sup>4</sup> Among the oxide ceramics for biomedical and dental applications, alumina and zirconia have been used for many years.<sup>5–8</sup> Aluminum oxide was introduced as a material for orthopedic bearings in the 1970s and has been the most widely used ceramic material due to its low cost and high hardness,<sup>9</sup> whereas biomedical grade zirconia was introduced 20 year ago with the purpose to solve the problem of alumina brittleness and the consequent potential failure of implants.<sup>10</sup> It is well known that alumina is chemically more stable but it is mechanically weaker than zirconia, and the phase changes or

\*miguel.bocanegra@cimav.edu.mx  
© 2012 The American Ceramic Society

transformation mechanism in zirconia produce a ceramic having much higher strength and fracture toughness than  $\text{Al}_2\text{O}_3$  and other oxides.<sup>11</sup> Nevertheless, the low-temperature degradation (aging) of yttria tetragonal zirconia polycrystal (Y-TZP) characterized by surface roughening and microcracking at the surface of the material, limits their range of use as a biomaterial.<sup>12</sup> Aging occurs by slow tetragonal-to-monoclinic phase transformation of grains on any surface in contact with water, or body fluid. Therefore, the uniform distribution of  $\text{Al}_2\text{O}_3$  in the  $\text{ZrO}_2$  matrix can suppress the low-temperature degradation of mechanical properties.<sup>13</sup> The combination of alumina and zirconia in different percentages could be a particular solution leading to obtain a new ceramic composite with improved mechanical properties over monolithic ceramic components.<sup>11</sup>

The demand of ceramics with excellent mechanical properties has led to an increased interest in the processing and characterization of fiber reinforced ceramic composite systems.<sup>14</sup> To improve the fracture resistance of ceramic materials, extensive studies have been done on the incorporation of ceramic whiskers into ceramic matrices to form a whisker-reinforced ceramic matrix composite.<sup>15</sup> Becher and Wei<sup>16</sup> and Wei and Becher<sup>17</sup> incorporated approximately 20 vol% of very strong microscopic SiC whiskers into a fine-grained ( $<2\ \mu\text{m}$ ) polycrystalline alumina matrix resulting in a threefold increase in fracture resistance. Many other investigations of the Y-TZP ceramic have shown improved fracture toughness with various alumina additions.<sup>18–20</sup>

Considering the increase of research and publications related to whisker toughening ceramics (WTC), to the knowledge of the authors no detailed research work has yet been published on the effect of the addition of low alumina whisker content in combination with alumina particulates on the fracture toughness in zirconia based ceramics. The trend today is to develop alumina-zirconia composites as an alternative to the monolithic zirconia and alumina. Although the clinical outcomes of the alumina and zirconia ceramic joints have been very satisfactory, the research efforts are still continuing with the aim to improve the joint performances. On these expectations, the main objective of this article is to combine the transformation toughening in  $\text{ZrO}_2$  ceramics with the addition of 2.5 wt% of alumina whiskers in an attempt to improve the fracture toughness and hardness in ATZ ceramic composites obtained by pressureless sintering offering a ceramic component with enhanced mechanical properties for

possible long-term applications in artificial joint components and dental applications considering that with the addition of  $\text{Al}_2\text{O}_3$  particles to zirconia, at least the aging kinetics can be reduced.<sup>10</sup> However, *in vitro* and *in vivo* assessments are necessary before these can be considered for future clinical applications inasmuch as new unexpected biological responses could occur.

## Experimental Methods

The starting materials used were,  $\alpha\text{-Al}_2\text{O}_3$  (Baikalox SM8; Baikowski Malakoff, Malakoff, TX; mean particle size 100 nm, purity  $>99.99\%$ , surface area  $10\ \text{m}^2/\text{g}$ ), MgO (500A; UBE Chemical, Ube, Japan; mean particle size 60 nm, purity  $>99.999\%$ , surface area  $32\ \text{m}^2/\text{g}$ ),  $\text{ZrO}_2 + 3\ \text{mol}\% \text{Y}_2\text{O}_3$  (thereafter abridged as TZ-3Y, Tosoh, Tokyo, Japan; mean particle size 75 nm, purity  $>99.99\%$ , surface area  $17\ \text{m}^2/\text{g}$ ), powders and  $\text{Al}_2\text{O}_3$  whiskers ( $2\text{--}4\ \text{nm} \times 2800\ \text{nm}$ , Aldrich, St. Louis, MO). To evade possible changes on the  $\text{Al}_2\text{O}_3$  whisker surfaces by dispersing agents, the starting materials such as  $\text{Al}_2\text{O}_3$  powder,  $\text{Al}_2\text{O}_3$  whiskers, and 3Y zirconia were used directly in their “as received” state without any pretreatment. A mixture of TZ-3Y with 30 wt%  $\text{Al}_2\text{O}_3$  (2.5 wt%  $\text{Al}_2\text{O}_3$  whiskers +  $\text{Al}_2\text{O}_3$  nanoparticles) was prepared.  $\text{Al}_2\text{O}_3$  whiskers were firstly dispersed in alcohol during 40 min using ultrasonic shaker to destroy the agglomeration state. Then,  $\text{Al}_2\text{O}_3\text{--MgO}$  (MgO content of 0.25 wt% as inhibitor of grain growth)–TZ-3Y nanopowders were added to the whiskers and the mixture was dispersed by magnetic stirring for about 24 h until all the solvent evaporated. The resulting dry mix was intensively ground in an agate mortar. Pure  $\text{Al}_2\text{O}_3$  and TZ-3Y ceramic samples were also prepared for comparison. A X-Ray diffractometer model X' Pert Pro (PANalytical, Almelo, The Netherlands), equipped with Cu  $K\alpha$  monochromatic radiation and  $\theta\text{--}2\theta$  geometry was used to identify possible monoclinic phase (*m*) on polished and fracture surfaces in ATZ nanocomposites containing alumina whiskers. The data were collected on the  $2\theta$  range from  $20^\circ$  to  $80^\circ$  at intervals of  $0.05^\circ\ 2\theta$  using a step-counting time of 10 s.

Green compacts were uniaxially consolidated at 50 MPa applied pressure in a steel die diameter 16 mm using an Elvec Hydraulic Press (ELVEC S.A. de C.V., México D.F., México) at a constant strain rate. The samples were sintered at  $1500^\circ\text{C}$  during 2 h in air at a heating rate of  $10^\circ\text{C}/\text{m}$  using a

$\text{ZrO}_2 + \text{Al}_2\text{O}_3$  mixture as bed powder. After sintering, the furnace was shut off and it was allowed to cool down. The density of sintered composites was measured using the Archimedes displacement method with distilled water as the suspending liquid. Then, the samples were ground and polished through SiC paper and then mirror polished by using diamond pastes of 0.5 and 0.25  $\mu\text{m}$  and subsequently thermally etched in air for 30 min at a temperature of 1350°C. A drop of the above dispersed  $\text{Al}_2\text{O}_3$  whiskers was deposited onto a copper sheet to be characterized.

The polished and fracture surfaces as well as the  $\text{Al}_2\text{O}_3$  whiskers were characterized by scanning electron microscopy (SEM; JEOL JSM 5800 LV, Tokyo, Japan, and FEG SEM; JEOL JMS 7000F) using 2 kV acceleration voltage. Transmission Electron Microscopy (TEM; JEOL-2200FS HR-FE-TEM) was also used to examine  $\text{Al}_2\text{O}_3$  whiskers. The average grain size was determined by using the linear intercept method measuring about 300 grains for each sample. Mechanical properties were determined by using Vickers hardness tester (Microhardness Tester FM-7, Future-Tech, Tokyo, Japan) on sintered samples. The cracks were introduced at a load of 1.0 kg held for 15 s. To avoid cracking or spalling around the Vickers impression which affect the hardness and fracture toughness measurements, lower indentation load was used. A total of 30 indents were made at the applied load and the average values of the diagonal lengths of indentation marks were obtained. The separation between neighboring indentations was more than four diagonal lengths of indentation impression following the standard ASTM C1327-99 for advanced ceramics.<sup>21</sup> The crack lengths were determined using an optical microscope Olympus PMG3 (by Olympus, Tokyo, Japan) and the indentation fracture toughness ( $K_{IC}$ ) was calculated using the formula given by Evans and Charles<sup>22</sup> as follows:

$$K_{IC} = 0.0752 \cdot P / C^{3/2} \quad (1)$$

where  $K_{IC}$  is the fracture toughness,  $P$  the load and  $C$  the crack length.

## Results and Discussion

Figures 1a and b illustrate the corresponding SEM micrographs of the “as received” and dispersed alumina whiskers showing agglomerates with different sizes and

shapes and an isolated and elongated whisker, respectively. On the other hand, Fig. 1c and d correspond to TEM micrographs of individual  $\text{Al}_2\text{O}_3$  whisker approximately 100 nm diameter  $\times$  300 nm length (c), and 300 nm diameter  $\times$  1.400 nm length (d). Note that whisker diameter dimensions are higher than those given by manufacturer.

The relative densities for all samples were greater than 94% of the theoretical density (see Table I). The low sintered density observed in the composite with additions of alumina whiskers compared to that of pure  $\text{Al}_2\text{O}_3$  and TZ-3Y ceramics could be attributed to the formation of some defects as consequence of the agglomeration state of the whiskers hindering full densification.

The Vickers hardness changes when both  $\text{Al}_2\text{O}_3$  particles and  $\text{Al}_2\text{O}_3$  whiskers are added to the  $\text{ZrO}_2$  (TZ-3Y) matrix, remain within our experimental errors. However, with the increase of zirconia content, the hardness of the composites diminishes suggesting that the zirconia addition changes the composite behavior. This assertion can be supported with the results of previous work<sup>23</sup> where the hardness is approximately constant for additions of alumina in zirconia up to 30 wt % in composites without additions of  $\text{Al}_2\text{O}_3$  whiskers. The fracture toughness was increased to 8% and 28% in the 27.5 wt%  $\text{Al}_2\text{O}_3$  particles + 2.5 wt%  $\text{Al}_2\text{O}_3$  (w) + 70 wt% TZ-3Y nanocomposite compared to monolithic TZ-3Y and composite free of alumina whiskers, respectively. The fracture toughness for the composite with additions of  $\text{Al}_2\text{O}_3$  whiskers was significantly higher than that obtained in pure  $\text{Al}_2\text{O}_3$  monolithic ceramic (approximately 62%). These behaviors are summarized in Table II.

On the other hand, based on commercial ceramic materials, the fracture toughness of whisker-reinforced ceramic composites is relatively high.<sup>24</sup> Taking into account that the yttria-stabilized tetragonal zirconia polycrystals (Y-TZP) reveal high fracture toughness, an alternate way to improve its mechanical properties is the addition of strong  $\text{Al}_2\text{O}_3$  whiskers. As was mentioned earlier, if clusters of whiskers remain during their processing, these will remain in the final ceramic as low density regions which in turn will degrade the final mechanical properties. In this context, several problems must be resolved to obtain a fully consolidated whisker toughened ceramics (WTCs) green compact. One of them is their agglomeration. These tend to form large clusters and their homogeneous

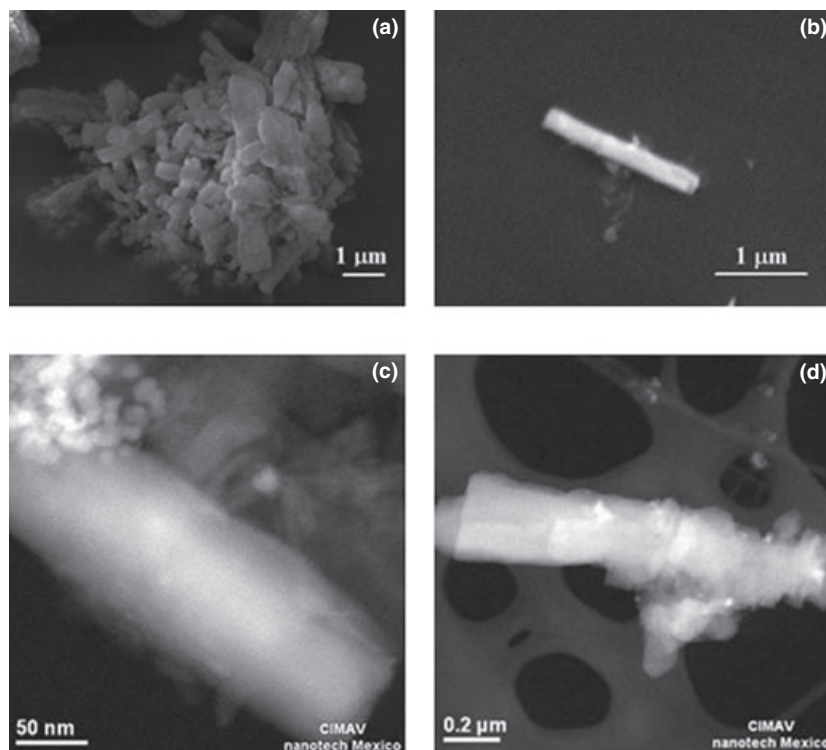


Fig. 1. SEM micrographs showing (a) the “as received”  $\text{Al}_2\text{O}_3$  whiskers, and (b) High magnification of  $\text{Al}_2\text{O}_3$  whiskers after dispersing them in alcohol showing an isolated and elongated  $\text{Al}_2\text{O}_3$  whisker. (c) and (d) are TEM images showing individual alumina whiskers.

**Table I. Sintered Densities of the Experimental Ceramics**

Composition	Relative density (%)
Pure $\text{Al}_2\text{O}_{3(\text{n})}$	98.0
30 wt% $\text{Al}_2\text{O}_{3(\text{n})}$ + 70 wt% TZ-3Y	96.0
27.5 wt% $\text{Al}_2\text{O}_{3(\text{n})}$ + 2.5 wt% $\text{Al}_2\text{O}_{3(\text{w})}$ + 70 wt% TZ-3Y	94.5
Pure TZ-3Y <sub>(n)</sub>	98.0

(n), nanoparticles; (w), whiskers.

incorporation to the ceramic matrix powder is very difficult tending to a low packing efficiency.<sup>25</sup>

The sintering of a powder compact in the presence of whiskers is sometimes difficult inasmuch as they could resist particle rearrangement owing to extensive sliding distances along whisker boundaries during sintering as well as high whisker aspect ratios, or ratios

above a critical volume fraction. The agglomerated particles formed by the whiskers can act as rigid inclusions avoiding the complete densification and homogeneity of the phase distribution. Similar observations has been reported by Yang and Stevens,<sup>26</sup> where large matrix particles localized at the intersection of whiskers welded the network firmly, which left interparticle porosity.

The reinforcement role of the  $\text{Al}_2\text{O}_3$  whiskers in Zirconia composite might affect the increase in hardness. However, for additions of 2.5 wt% of whiskers, the hardness is practically the same compared to the monolithic TZ-3Y considering the experimental error. The higher standard deviation in the composites with and without whiskers addition compared to pure TZ-3Y (Table II) could be related to the final porosity present in each sample. Therefore, a decrease in the porosity percentage and their distribution leads to improvement in hardness. It is well known that the hardness and the fracture toughness values of ceramics can be reported as a function of the grain size. A decrease in hardness for sintered  $\text{ZrO}_2\text{--Al}_2\text{O}_3$  compos-

**Table II. Mechanical Properties of the Experimental Ceramics**

Composition	Vickers hardness (GPa)	Fracture toughness ( $\text{MPa}\cdot\text{m}^{1/2}$ )
Pure $\text{Al}_2\text{O}_{3(\text{n})}$	$21.8 \pm 1.7$	$4.2 \pm 0.4$
30 wt% $\text{Al}_2\text{O}_{3(\text{n})}$ + 70 wt% TZ-3Y	$13.4 \pm 1.3$	$5.4 \pm 1.8$
27.5 wt% $\text{Al}_2\text{O}_{3(\text{n})}$ + 2.5 wt% $\text{Al}_2\text{O}_{3(\text{w})}$ + 70 wt% TZ-3Y	$13.8 \pm 1.8$	$6.9 \pm 0.8$
Pure TZ-3Y <sub>(n)</sub>	$13.7 \pm 0.5$	$6.4 \pm 0.4$

(n), nanoparticles; (w), whiskers.

ites is attributed to increase of the grain size according to findings reported by Daguno *et al.*,<sup>27</sup> meanwhile Suzuki *et al.*,<sup>28</sup> reported that the Vickers hardness is directly correlated with porosity in the former sintering stage although in the latter sintering stage there is a correlation with the grain size. In the present investigation, a hardness  $>13$  GPa (which is higher than 12 GPa of the conventional Y-TZP<sup>13</sup>), was obtained in the composite with 2.5 wt% whiskers content and an average grain size of  $0.40 \pm 0.17$   $\mu\text{m}$  which was lower than  $1.3 \pm 0.5$  and  $0.6 \pm 0.1$   $\mu\text{m}$  obtained in “as sintered” alumina and zirconia monoliths, respectively. Therefore,

the refinement of the microstructure maintaining approximately constant the hardness but increasing fracture toughness (Table II) is very possible at low amounts of  $\text{Al}_2\text{O}_3$  particles and whiskers in TZ-3Y.

The fracture surfaces of 27.5 wt%  $\text{Al}_2\text{O}_{3(\text{n})}$  + 2.5 wt%  $\text{Al}_2\text{O}_{3(\text{w})}$  + 70 wt%  $\text{ZrO}_2$  (TZ-3Y) and 30 wt%  $\text{Al}_2\text{O}_{3(\text{n})}$  + 70 wt%  $\text{ZrO}_2$  (TZ-3Y) nanocomposites are shown in Fig. 2a and b, respectively. The high fracture toughness ( $6.9 \pm 0.8$   $\text{MPa}\cdot\text{m}^{1/2}$ ) obtained in the composite with additions of alumina whiskers could be attributed to the fracture mode which can be classified as mainly intergranular (many pits present on

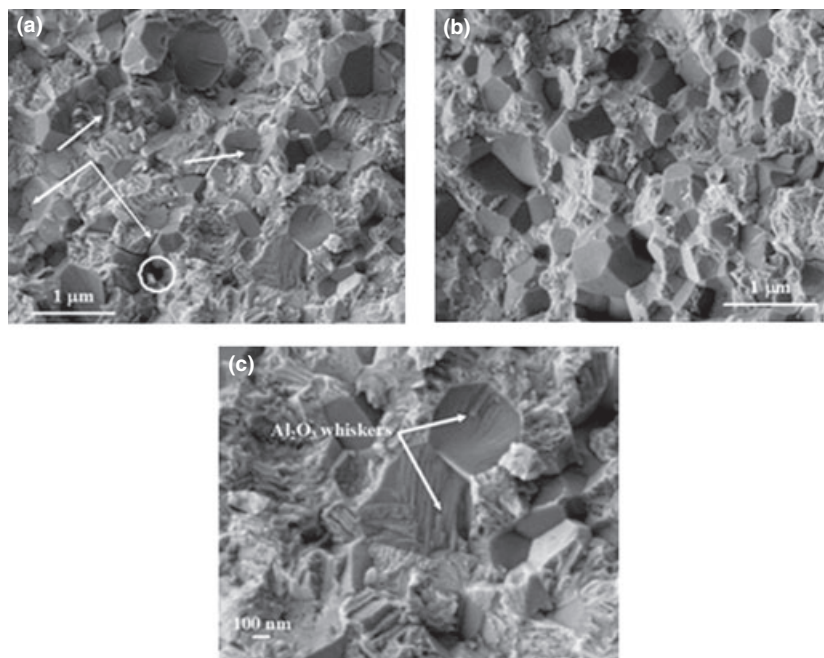


Fig. 2. SEM micrographs of fracture surface of 27.5 wt%  $\text{Al}_2\text{O}_{3(\text{n})}$  + 2.5 wt%  $\text{Al}_2\text{O}_{3(\text{w})}$  + 70 wt%  $\text{ZrO}_2$  (TZ-3Y) (a), 30 wt%  $\text{Al}_2\text{O}_{3(\text{n})}$  + 70 wt%  $\text{ZrO}_2$  (TZ-3Y) (b) nanocomposites. Higher magnification of Fig. 2a is shown in (c). Arrow marks and circle are explained in text.



the fracture surface) and partially transgranular as can be observed in Fig. 2a, where the roughness in this fracture surface is increased compared to the relatively smooth fracture surface shown in Fig. 2b corresponding to the ceramic composite free of  $\text{Al}_2\text{O}_3$  whiskers (fracture toughness of  $5.4 \pm 1.8 \text{ MPa m}^{1/2}$ ). Micro-cracking (arrow marks in Fig. 2a) as well as isolated holes resulting from alumina whiskers pull out (see circle mark in Fig. 2a) were identified as possible toughening mechanisms. It is well known that the intergranular fracture mode will improve the fracture toughness of the composite by crack deflection mechanism.<sup>29,30</sup> On the other hand, in the Fig. 2c (higher magnification of the Fig. 2a) are shown some  $\text{Al}_2\text{O}_3$  whiskers embedded in the alumina grains suggesting that the length of the embedded whiskers and their orientation and position respect to the crack planes, could strongly influence the bridging and pullout mechanisms. The improvement in fracture toughness can be a direct consequence of an increase in crack deflection

(high deviation angles) as can be seen in Fig. 3a (high magnification of one arm of an indented impression in the same figure). Conversely, low fracture toughness in the composite free of  $\text{Al}_2\text{O}_3$  whiskers is explained by the decreasing in number of crack deviations as well as deflection angles (high magnification of the square in Fig. 3b) suggesting that the crack deflection mechanism is less effective in the toughening process.<sup>31</sup> In the composite with alumina whisker addition (Fig. 3a), the measured crack length was slightly smaller than that in the composite free of whiskers (Fig. 3b) suggesting an improvement in fracture toughness. It is also observed that in the composite without whiskers addition, the portion of intragranular fracture (arrow marks in Fig. 3b) is higher than that of composite containing  $\text{Al}_2\text{O}_3$  whiskers (arrow marks in Fig. 3a) where the fracture intergranular mode was predominant. On the other side, it is very important to note that some “nanodefects” in the alumina whiskers could contribute to enhance the fracture toughness creating structural

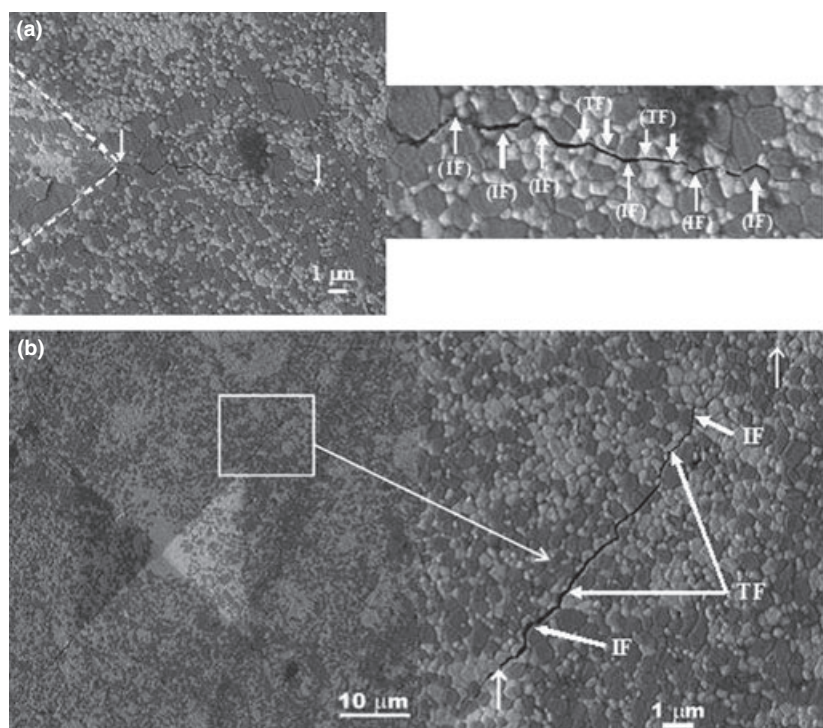


Fig. 3. SEM of typical hardness impressions and high magnification of one arm of an indented 27.5 wt%  $\text{Al}_2\text{O}_{3(n)}$  + 2.5 wt%  $\text{Al}_2\text{O}_{3(w)}$  + 70 wt%  $\text{ZrO}_2$  (TZ-3Y) (a), and 30 wt%  $\text{Al}_2\text{O}_{3(n)}$  + 70 wt%  $\text{ZrO}_2$  (TZ-3Y) (b) nanocomposites. The arrow marks indicate the beginning and final of the crack and dashed lines in Fig. 3a correspond to the contour of the Vickers impression. IF = Intergranular fracture, TF = Intragranular fracture.

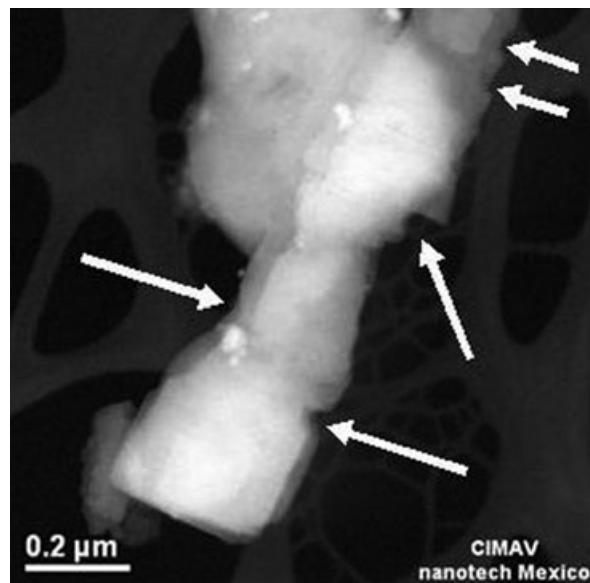


Fig. 4. TEM image of the  $\text{Al}_2\text{O}_3$  whisker. Arrow marks explained in text.

anchors (arrow marks in in Fig. 4) that improve the connectivity between the  $\text{Al}_2\text{O}_3$  whiskers and the matrix. In spite of scatter in the data, the obtained ZTA composite with additions of 2.5 wt% of whiskers reached a maximum fracture toughness of  $6.9 \pm 0.8 \text{ MPa m}^{1/2}$  which is statistically comparable to  $6.4 \pm 0.4 \text{ MPa m}^{1/2}$  obtained for pure TZ-3Y zirconia. Therefore, the fracture toughness determined for ZTA composite with addition of whiskers is, however, higher than that in ZTA free of  $\text{Al}_2\text{O}_3$  whiskers. Although the absolute toughness values obtained by the conventional indentation method could be overestimated, this technique has proved to be able to provide consistent evidence of the toughening role of alumina whiskers.

In ceramic composites with alumina whiskers contents and in the vicinity of a whisker, the propagation energy of the advancing crack could undoubtedly be dissipated and therefore, the crack deflected or pinned. On the other side, depending on whether the advancing crack interacts with a porous or dense whisker, it is also highly probable to obtain different fracture toughness values in the same ceramic depending of the orientation of these  $\text{Al}_2\text{O}_3$  whiskers. An important contribution to the fracture toughness improvement in the ceramic composite with 2.5 wt%  $\text{Al}_2\text{O}_3$  whiskers has been the phase transformation from tetragonal (*t*) to monoclinic (*m*) phase on the fracture surface as was

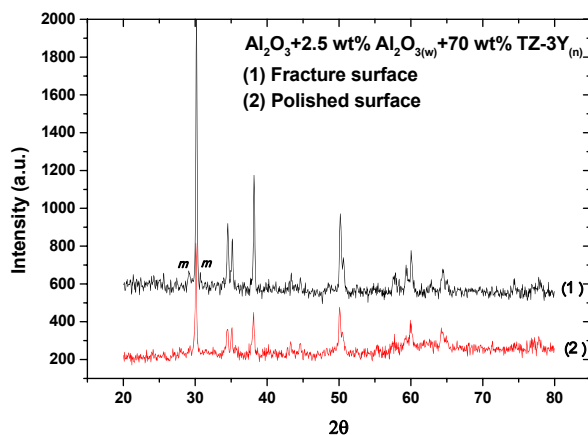


Fig. 5. XRD analysis on the polished and fracture surface of the 27.5 wt%  $\text{Al}_2\text{O}_{3(n)}$  + 2.5 wt%  $\text{Al}_2\text{O}_{3(w)}$  + 70 wt%  $\text{ZrO}_2$  (TZ-3Y) composite.

argued by Nevarez *et al.*<sup>32</sup> This phase transformation is a consequence of the different thermal expansion coefficients of the  $\text{ZrO}_2$  (TZ-3Y) matrix ( $10.3 \times 10^{-6}/^\circ\text{C}$ ) and  $\text{Al}_2\text{O}_3$  ( $8.1 \times 10^{-6}/^\circ\text{C}$ ) grains or alternately to matrix microcrack formation prior to or during fracture of the ceramic composite (arrow marks in Fig. 2a). This can be supported by the in Fig. 5 where is shown the X-ray diffraction (XRD) patterns corresponding to the polished and fracture surfaces of the ZTA composite with alumina whiskers addition. From this Fig. 5 is observed a slight increase in monoclinic (*m*) zirconia phase transformed from tetragonal (*t*) phase during fracture (pattern labeled as 1 in Fig. 5) indicating a contribution to the toughening by phase transformations. Similar results have been reached by Wang *et al.*<sup>3</sup>

## Conclusions

In the present study, the Vickers hardness and fracture toughness of  $\text{Al}_2\text{O}_{3(n)}$  + 70 wt%  $\text{ZrO}_2$  (TZ-3Y)<sub>n</sub> nanocomposites with addition of 2.5 wt%  $\text{Al}_2\text{O}_3$  whiskers were studied. It is concluded that:

1. Sintered densities >95% of theoretical density were obtained in the composites as well as pure  $\text{Al}_2\text{O}_3$  and TZ-3Y monolithic ceramics.
2. Hardness higher than 13 GPa and a maximum fracture toughness of  $6.9 \text{ MPa m}^{1/2}$  with an average grain size of  $0.4 \pm 0.17 \mu\text{m}$  were reached. This fracture toughness was increased 62%, 28%, and

7% over pure  $\text{Al}_2\text{O}_3$ , the composite without additions of whiskers, and pure TZ-3Y for medical applications, respectively.

3. Crack deflection mechanism was more efficient for ceramic composites in the presence of alumina whiskers compared to free whiskers sample.
4. The phase transformation of tetragonal (*t*) to monoclinic phase (*m*) on the fracture surface could also contribute to the increase in fracture toughness.  $\text{Al}_2\text{O}_3$  whiskers could be used to improve the fracture toughness of ATZ composites without affecting other intrinsic properties. Following this, the lower amounts of  $\text{Al}_2\text{O}_3$  whiskers added to our ATZ composites will open the door to several applications in the field of medical and dental applications considering that with a decrease  $\text{ZrO}_2$  content in the composite the prior observed material degradation by the aging mechanism at low temperature can be reduced or avoided. However, a more detailed work is required to understand the role of whiskers in the reinforcement of ATZ nanocomposites.

## Acknowledgments

The authors express their appreciation to Wilber Antúnez and Karla Campos for invaluable SEM work as well as A. Nevarez R. for his assistance in hardness and fracture toughness measurements. Special acknowledgement must be extended to Enrique Torres M. and Cesar Leyva P. for the assistance with the XRD and TEM studies, respectively.

## References

1. Y. Ye, J. Li, H. Zhou, and J. Chen, "Microstructure and Mechanical Properties of Ytria-Stabilized  $\text{ZrO}_2/\text{Al}_2\text{O}_3$  Nanocomposite Ceramics," *Ceram. Int.*, 34 1797–1803 (2008).
2. M. H. Maneshian and M. K. Banerjee, "Effect of Sintering on Structure and Mechanical Properties of Alumina–15 vol% Zirconia Nanocomposite Compacts," *J. Alloy. Compd.*, 493 613–618 (2010).
3. X. Wang, J. Tian, X. Yu, Y. Shan, Z. Liu and Y. Yin, "Effect of Microstructure on the Fracture Behavior of Micro-Nano ZTA Composite," *Mat. Chem. Phys.*, 112 213–217 (2008).
4. O. Vasylykiv, Y. Sakka, and V. V. Skorokhod, "Low-Temperature Processing and Mechanical Properties of Zirconia and Zirconia–Alumina Nanoceramics," *J. Am. Ceram. Soc.*, 86 299–304 (2003).
5. J. P. Garino, "Modern Ceramic-on-Ceramic Total Hip Systems in the United States: Early Results," *Clin. Orthop. Relat. R.*, 379 41–47 (2000).
6. D. Hannouche, M. Hamadouche, R. Nizard, P. Bisot, A. Meunier, and L. Sedel, "Ceramics in Total Hip Replacement," *Clin. Orthop. Relat. R.*, 430 62–71 (2005).
7. M. Agaki, T. Nakamura, Y. Matsusune, T. Ueo, K. Nishijyo and E. Ohnishi, "The Surface Total Knee Replacement: A Unique Design for Flexion. Four-to-Nine-Year Follow-Up Study," *J. Bone Joint Surg.*, 82 1626–1633 (2000).
8. K. Yasuda, N. Miyagi, and K. Kaneda, "Low Friction Total Knee Arthroplasty with the Alumina Ceramic Condylar Prosthesis," *B. Hosp. Joint Dis. Ort.*, 53 15–21 (1993).
9. S. Yip, "The Strongest Size," *Nature*, 391 532–533 (1998).
10. J. Chevalier, "What Future for Zirconia as a Biomaterial?" *Biomaterials*, 27 535–543 (2006).
11. S. Affatato, M. Goldoni, M. Testoni, and A. Toni, "Mixed Oxides Prosthetic Ceramic Ball Heads. Part 3: Effect of the  $\text{ZrO}_2$  Fraction on the Wear of Ceramic on Ceramic Hip Joint Prostheses. A Long-Term *In Vitro* Wear Study," *Biomaterials*, 22 717–723 (2001).
12. R. Benzaid, *et al.*, "Fracture Toughness, Strength and Slow Crack Growth in a Ceria Stabilized Zirconia-Alumina Nanocomposite for Medical Applications," *Biomaterials*, 29 3636–3641 (2008).
13. Y. Zhang, J. Chen, L. Hu, and W. Liu, "Pressureless-Sintering Behavior of Nanocrystalline  $\text{ZrO}_2\text{--Y}_2\text{O}_3\text{--Al}_2\text{O}_3$  System," *Mat. Lett.*, 60 2302–2305 (2006).
14. T. Leutbecher and D. Hulsberg, "Oxide Fiber Reinforced Glass: a Challenge to New Composites," *Adv. Eng. Mater.*, 2 93–99 (2000).
15. X. Zhang, L. Xu, W. Han, L. Weng, J. Han and S. Du, "Microstructure and Properties of Silicon Carbide Whisker Reinforced Diboride Ultra-High Temperature Ceramics," *Solid State Sci.*, 11 156–161 (2009).
16. P. F. Becher and G. C. Wei, "Toughening Behavior in SiC-Whisker-Reinforced Alumina," *J. Am. Ceram. Soc.*, 67 C267–C269 (1984).
17. G. C. Wei and P. F. Becher, "Development of SiC-Whisker-Reinforced Ceramics," *Am. Ceram. Soc. Bull.*, 64 298–304 (1985).
18. G. Dransman, R. Steinbrech, A. Pajares, F. Guiberteau, A. Domínguez-Rodríguez and A. Heuer, "Indentation Studies on  $\text{Y}_2\text{O}_3$ -Stabilized  $\text{ZrO}_2$ : II, Toughness Determination from Stable Growth of Indentation-Induced Cracks," *J. Am. Ceram. Soc.*, 77 1194–1201 (1994).
19. J. Adams, R. Ruh, and K. Mazdiyasi, "Young's Modulus, Flexural Strength, and Fracture of Ytria-Stabilized Zirconia Versus Temperature," *J. Am. Ceram. Soc.*, 80 903–908 (1997).
20. L. Ruiz and M. J. Readey, "Effect of Heat Treatment on Grain Size, Phase Assemblage and Mechanical Properties of 3 mol% Y-TZP," *J. Am. Ceram. Soc.*, 79 2331–2340 (1996).
21. American Society for Testing of Materials, Designation C 1327-99 Standard test method for Vickers indentation hardness of advanced ceramics. In: Annual Book of ASTM Standard 15.01, Philadelphia: ASTM; 1999.
22. A. G. Evans and E. A. Charles, "Fracture Toughness Determinations by Indentation," *J. Am. Ceram. Soc.*, 59 371–372 (1976).
23. A. Nevarez-Rascon, A. Aguilar-Elguézabal, E. Orrantia, and M. H. Bocanegra-Bernal, "On the Wide Range of Mechanical Properties of ZTA and ATZ Based Dental Ceramic Composites by Varying the  $\text{Al}_2\text{O}_3$  and  $\text{ZrO}_2$  Content," *Int. J. Refract. Mater. Met. H*, 27 962–970 (2009).
24. J. M. Roberts, J. P. Singh, and R. O. Scattergood, "Microstructure and Properties of Alumina-Whisker-Reinforced Tetragonal Polycrystal Matrix Composites," CONF-910162-1, 1991.
25. M. Bengisu and O. T. Inal, "Whisker Toughening Of Ceramics: Toughening Mechanisms, Fabrication and Composite Properties," *Annu. Rev. Mater. Sci.*, 24 83–124 (1994).
26. M. Yang and R. Stevens, "Microstructure and Properties of SiC Whisker Reinforced Ceramic Composites," *J. Mater. Sci.*, 26 726–736 (1991).
27. J. K. M. F. Daguan, C. Santos, R. C. Souza, R. M. Balestra, K. Strecker, and C. N. Elias, "Properties of  $\text{ZrO}_2\text{--Al}_2\text{O}_3$  Composite as a Function of Isothermal Holding Time," *Int. J. Refract. Mater. Met. H*, 25 374–379 (2007).
28. H. Y. Suzuki, K. Shinosaki, H. Kuroi, and S. Tashima, "Sintered Microstructure and Mechanical Properties of High Purity Alumina Ceramics made by High-Speed Centrifugal Compaction Process," *Key Eng. Mater.*, 159–160 87–192 (1999).



29. M. Guazzato, M. Albakry, S. P. Ringer, and M. V. Swain, "Strength, Fracture Toughness and Microstructure of a Selection of All-Ceramic Materials. Part I. Pressable and Alumina Glass-Infiltrated Ceramics," *Dental Mater.*, 20 441–448 (2004).
30. J. I. Thompson, K. J. Anusavice, B. Balasubramaniam, and J. J. Mecholsky, "Effect of Microcracking on the Fracture Toughness and Fracture Surface Fractal Dimension of Lithia-Based Glass-Ceramics," *J. Am. Ceram. Soc.*, 78 3045–3049 (1995).
31. A. Celli, A. Tucci, and L. Esposito, "Quantitative Evaluation by Fractal Analysis of Indentation Crack Paths in  $Si_3N_4$ -SiCw Composites," *J. Eur. Ceram. Soc.*, 19 441–449 (1999).
32. A. Nevarez-Rascón, A. Aguilar-Elguézabal, E. Orrantia, and M. H. Bocanegra-Bernal, " $Al_2O_{3(w)}-Al_2O_{3(n)}-ZrO_2$  (TZ-3Y)<sub>n</sub> Multi-Scale Nanocomposite: An Alternative for Different Dental Applications?" *Acta Biomater.*, 6 563–570 (2010).